IMAV2017-32
https://www.imavs.org/pdf/imav.2017.32



# Development and Design Methodology of an Anti-Vibration System on Micro-UAVs

Zhenming Li[1], Mingjie Lao[2], Swee King Phang[2]*, Mohamed Redhwan Abdul Hamid[2], Kok Zuea Tang[3], and Feng Lin[2]
[1]Mechanical Engineering, National University of Singapore, Singapore
[2]Temasek Laboratories, National University of Singapore, Singapore
[3]Electrical and Computer Engineering, National University of Singapore, Singapore

ABSTRACT

As the potential applications of unmanned aerial vehicles (UAVs) are growing, more sensors are installed on-board. Mechanical vibration of the UAV, which greatly hinders the accuracy of its on-board sensors, becomes an increasingly important issue. In this manuscript, an anti-vibration framework on micro-UAVs is proposed. The vibration sources of the UAV will be investigated and identified. Then, several selections of hardware dampers are tested along with a digital low-pass filter on actual UAV. With the results from different case studies, a criteria of damper selection for micro-UAV is built to serve as a guideline for further practice.

## 1 INTRODUCTION

An unmanned aerial vehicle (UAV), commonly known as a drone, may be controlled by a remote-pilot or operated autonomously without human intervention. Due to its small size and remoteness during operation, modern miniature-UAVs are now widely used in both commercial and military aspects to fulfill the needs in different scenarios [1]. One of the popular research areas is on scouting of remote areas with limited GPS reception (such as indoor or foliage environment) through on-board cameras for localization mean [2].

To realized such applications, useful data are often collected from the sensors such as inertial measurement unit (IMU) and camera images at low frequencies (1-20 Hz approximately) to realize navigation or localization algorithms by estimating the UAV position and bearing [3, 4, 5]. The accuracy of these data is important for the flight control system to ensure good performance during flights. One major factor hindering the accuracy of these data is the mechanical vibration of the UAV during flights. Among the multiple causes to the vibration problem, rotating rotors and structure vibration on its natural frequencies are of most concern [6, 7].

Fortunately, these vibrations are usually recorded as higher frequency signals by IMU and they tend to pollute the useful signals at low frequency through the phenomenon of aliasing. Under such effect, higher frequency signals are observed as lower frequency signals causing inaccurate data. To avoid aliasing effect, one common method is to sample the data with the rate of at least 2 times of the maximum frequency of the signal. However, there is a limit to how fast the sampling frequency is and the relative high frequency of vibration generated signals will continue to impair the accuracy of the useful signals. Insufficient damping to such vibrations will also likely result in sensor drifting such as coning and sculling motion which is the condition where the output received by gyroscope or accelerometer becomes more inaccurate over time.

*Email address: skphang@nus.edu.sg

Figure 1: T-Lion developed at TL@NUS

Acknowledging the importance of implementing anti-vibration measures on-board, different dampers and isolators have been considered and recommended for vibration minimization. For instants, Kyosho Zeal sheet and its performances have been briefly studied in [8]; Wire-rope isolators and rubber dampers for minimum vibration effects towards data logging during flight has been discussed in [9]. In this manuscript, theoretical research will be done on a selections of dampers and isolators for the best anti-high-frequency vibrations to be used in UAV. The results will be further verified by state-of-the-art bench tests and UAV flight trials.

The UAV to be used to verify the proposed anti-vibration system is an in-house UAV developed by the Temasek Laboratories at the National University of Singapore (TL@NUS), codenamed T-Lion (see Fig. 1). It weighs 3 kg and is capable to carry additional 2 kg payload. On-board system to be isolated from the UAV structural vibration consists of a full IMU sensor suite weighs 120 g.

The manuscript is divided as follows: Section 1 will be

IMAV2017-32
https://www.imavs.org/pdf/imav.2017.32



given as introduction to this work; Section 2 lists the relevant theoretical frameworks involved in the study; Section 3 discusses the sources of vibrations in UAV; case studies of selected dampers are examined in Section 4; results verification via flight trials will be shown in Section 5 while concluding remarks will be made in the last Section.

## 2 Theoretical Frameworks

### 2.1 Vibration Damping and Vibration Isolation

Isolators are used to lower the natural frequency of the system to below the excitation (or disturbing) frequency (which in this case, the vibration frequency created by motors). Ultimately, the aim is to keep these two frequencies out-of-sync by 180° so that to avoid effects such as resonance. On the other hand, dampers are used to remove mechanical energy from disturbing vibration out of the system by absorbing the energy and converting to other forms of energy such as heat [10]. Normally, anti-vibration devices available in the market are both isolators and dampers. For simplicity, these are referred as dampers in this paper.

### 2.2 Transmissibility Curve

For effective vibration isolation from undesired high frequency, damper would need to have a natural frequency at least less than 50% of the lowest disturbing frequency, and optimally, less than 71%. In other words, the ratio of disturbing frequency over natural frequency is more than $\sqrt{2}$. This can be explained by transmissibility which is defined as the ratio of force transmitted through the suspension apparatus to force applied by vibration and it can be calculated through

$$T = \left|\frac{A_o}{A_i}\right| \equiv \left|\frac{a_o}{a_i}\right| \equiv \left|\frac{F_o}{F_i}\right|, \quad (1)$$

where $A_o$ and $A_i$ are the amplitudes for output and input respectively, $a_o$ and $a_i$ are the accelerations for output and input respectively, $F_o$ and $F_i$ are the forces for output and input (applied and transmitted) respectively [11].

Vibrations can never be completely removed from the system, i.e., $T \neq 0$ and hence minimizing this ratio for a specific frequency range is the goal of vibration isolation. Transmissibility curve can be divided into three regions: no effect region ($T = 1$), amplification region ($T > 1$), and isolation region ($T < 1$). In general, it is highly desirable to have the natural frequency of the damper as far apart as possible from the disturbing frequency to achieve effective vibration isolation. In general, isolation efficiency increases as the transmissibility decreases along increasing system frequency.

### 2.3 Static Deflection

Static deflection is how much the damper deflects when it is subjected to the static weight of the equipment it carries. In general, the larger the static deflection that the damper has before damping process, the better isolation effect can be achieved. In a single degree-of-freedom (DoF) system, natural frequency and static deflection are estimated to have an inverse linear relationship; larger static deflection will have a lower system natural frequency, and vice versa. As mentioned earlier, lower natural frequency leads to a larger separation from the disturbing frequency, thus better isolation efficiency. Therefore, it is important to use soft, flexible dampers for light damping mass to ensure a fair amount of static deflection is present.

### 2.4 Damper Selection Criteria

Judging from the above-mentioned characteristics, a few essential criteria for selecting dampers to be used in our studies are

1. Electrical insulator to avoid short-circuit;
2. Soft and flexible;
3. Natural frequency outside UAV structural resonance zone;
4. Low compression set and low creep;
5. Good resistance to outdoor conditions; and
6. Easy installation and adjustment.

## 3 Source of Vibration

Two main sources of high amplitude vibrations come from the rotating rotors, which has the same frequency to the rotating rate, and structural natural frequency vibrations, which the frequencies depend on the UAV structure. For T-Lion UAV, the rotors rotates at approximate 50 revolutions per second, which translates to 50 Hz vibration on the UAV. This section will be divided into two parts, where the structural natural frequencies will be studied in a simulation and the overall vibrations over a large frequency band will be obtained through experimental data with actual flight.

### 3.1 Structural Vibration Analysis

The T-Lion UAV is modeled in SolidWorks simulation, with the actual material properties assigned to each part of the simulated model. Frequency analysis on the model was carried out and vibration frequencies with significant impact are recorded as follows:

1. There are obvious high magnitude vibrations on $x$- and $y$-directions at 39.90 Hz (see Fig. 2 for mode shape visualization), and on $z$-direction at 80.48 Hz. From the simulation result, they are mainly caused by the hanging payload of T-Lion UAV below the UAV central region. It is also observed that similar behaviour also exists at 160.17 Hz and 321.82 Hz, which strongly suggested that they are the 3rd and 4th mode natural frequencies of the payload; and
2. Several small amplitude vibrations are observed between 100 to 200 Hz with lesser than 1 mm amplitude

**IMAV2017-32**
https://www.imavs.org/pdf/imav.2017.32



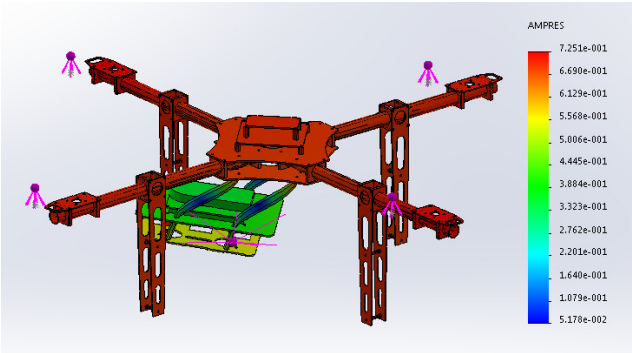


Figure 2: Mode shape of T-Lion at 39.9 Hz

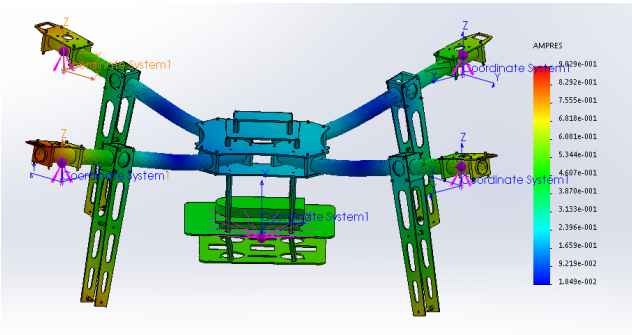


Figure 3: Mode shape of T-Lion at 109.88 Hz

(see Fig. 3 for mode shape visualization). A strong vibration of 3.15 mm amplitude is also observed at frequency of 273.16 Hz. They are most likely the structural natural frequencies of the UAV due to extending arms and components.

### 3.2 *Actual Flight Data*

To verify the vibration frequency of the UAV structure, an actual flight trial was carried out where the T-Lion was commanded to hover for several seconds in the air. An additional IMU sensor, the ADIS IMU was installed to the UAV for higher sampling rate of more than 800 Hz. With this sensor, acceleration data can be collected and converted to frequency domain with a frequency range up to 400 Hz. Experiments are designed to identify and examine different vibration signals and their corresponding vibration locations of the UAV.

Result in Fig. 4 shows that there is significant amount of vibration signals at high frequencies between 40 Hz to 400 Hz. Their magnitudes are large and thus cannot be neglected. By comparing the frequency response of the actual system with the simulated results above, vibrations of the UAV can be divided into 3 parts, demarcated clearly in Fig. 4:

1. A: These low frequency vibrations (approximately 40 Hz at $x$- and $y$-directions, approximately 80 Hz at $z$-direction) correspond to the vibrations at the payload of the UAV where the battery and certain weight source were located at the bottom of the UAV;
2. B: Vibration signals at B is originated from the rotating rotors at approximate 50 Hz; and
3. C: Vibration of the structure of UAV, mainly on the platform and the extension arms.

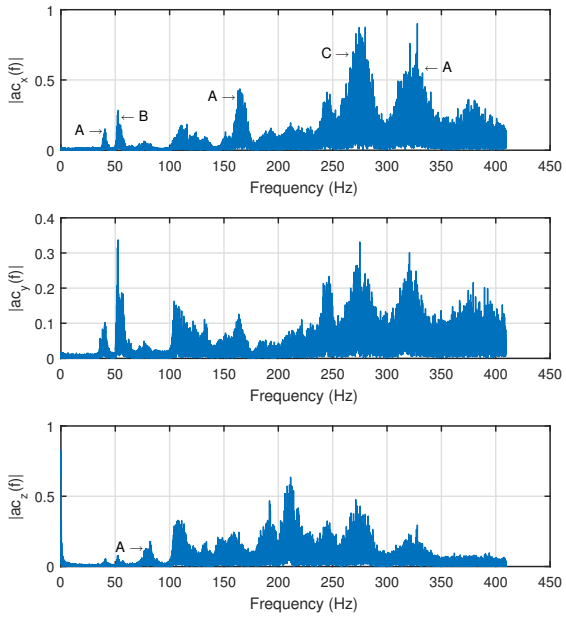


Figure 4: Vibration of T-Lion UAV measured by ADIS IMU

These vibration frequency peaks are rather consistent to our simulated results. It is concluded that structural vibrations are mainly high frequency signals, and some of them are so high that low-cost IMU sensor (with sampling rate below 100 Hz) would not detect them. They are undesired and thus dampers will be designed to filter them.

## 4 Case Studies

According to the damper selection criterion discussed in Section 2, four dampers have been selected for performance evaluations. The dampers can be visualized in Fig. 5.

### 4.1 *Silicone Ball Damper*

Silicone ball damper has similar functionality to the rubber damper, but it is made by better material. In general, silicone damper is softer than rubber damper leading to larger static deflection, which is preferable to reduce vibrations. However, it is difficult to install and to make changes to the damper on UAV due to its complicated installation mechanism. Furthermore, it requires high damping weight ($>$ 200 g) for efficient damping while the damping mass for T-Lion

**IMAV2017-32**
https://www.imavs.org/pdf/imav.2017.32



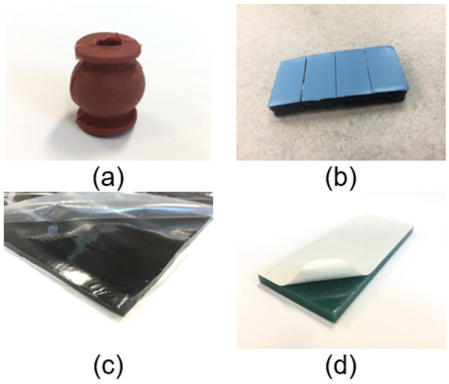


Figure 5: (a) Silicon Ball; (b) Silicon Foam; (c) Sorbothane sheet; and (d) Kyosho Zeal sheet

UAV is too light for this requirement (120 g). This option is thus discarded and will not be further discussed.

### *4.2 Silicone Foam*

Silicone Foam is the softest and the most flexible damper among all. Therefore, it is possible to damp a light weight IMU alone without the need to add extra mass. However, it may have very low natural frequency and eventually cause resonance with the useful signals at low frequency. On top of that, it breaks easily and thus not suitable to reuse.

### *4.3 Kyosho Zeal and Sorbothane 30 Durometer Sheets*

Kyosho Zeal sheet and Sorbothane 30 Durometer sheet are most used tape dampers recognized by many studies and experiments. They are easy to install and relatively soft to accommodate light masses. These can also be installed by clamping the mass in between two pieces of pads and compressing them to about 80% of its original thickness. This installation method enables the UAV to do inverse flying without compromising on damping. Kyosho Zeal sheet is relatively softer than Sorbothane 30 Durometer sheet, but their performance is comparable. However, these sheets have relatively higher compression set.

### *4.4 Damper Performances*

Using vibration table, static vibration tests have been done to verify the dampers performances subjecting to vibrations for a frequency range from 10 to 300 Hz. The actual loading on T-lion UAV is 120 g in total, which translates to 30 g per damper. Here, the stimulated damping mass used is 30 g to be consistent to the actual UAV load mass. Different dimensions are tested for selected dampers. Fig. 6 shows an example of the set-ups of the system on vibration table.

With Equation 1, transmissibility of each damper can be calculated with output and input acceleration data collected. Transmissibility curve for each damper is obtained by plotting the calculated transmissibilities with its corresponding frequencies. Observed from the results shown in Fig. 7, there

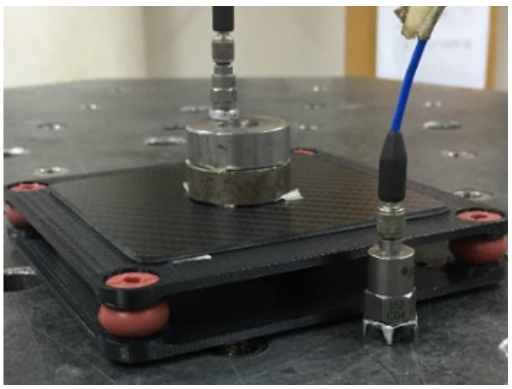

Figure 6: Vibration test setup on vibration table

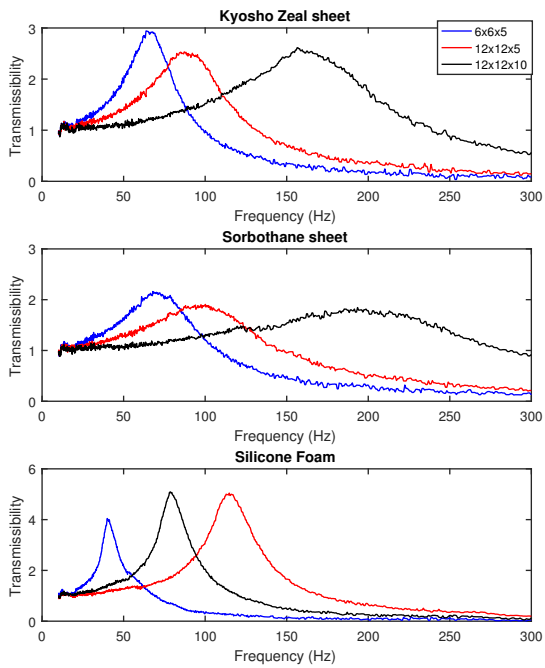


Figure 7: Transmissibility curve with different dimensions for Kyosho Zeal sheet, Sorbothane sheet, and Silicone foam

**IMAV2017-32**
https://www.imavs.org/pdf/imav.2017.32



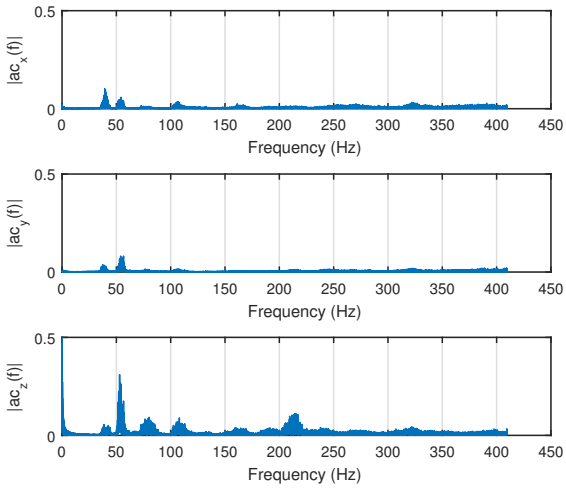


Figure 8: Vibration generated in actual UAV flight recorded by ADIS IMU sensor

is a clear shifts of the transmissibility curve towards the left when the smaller dampers are used, and this results to lower natural frequency of the damper. Ideally, the lower the natural frequency of the damped system, the better the isolation damper provides for system with high disturbing frequency.

Despite Silicone Foam has the lowest natural frequency, its high flexibility makes it sensitive to disturbances which worsens its performance. Overall, Kyosho Zeal Sheet has the best performance among the selections.

Its effect can be further proven by ADIS IMU testing as discussed earlier. Fig. 8 shows that almost all magnitudes of vibrations are reduced after a Kyosho Zeal sheet is installed to damp the sensor. Noted that for the vibrations at higher frequencies, the reduction is up to 96.8%. Also, as expected, motor noise at around 50 Hz is magnified as suggested in the transmissibility curve shown previously. However, this does not affect its effectiveness in minimizing vibrations at higher frequencies.

## 5 Flight Experiments

As Kyosho Zeal sheet was found to be best suited to damp the on-board sensors of weight 30 g each (120 g in total) from the previous section, the on-board system which includes IMU sensors were mounted on Kyosho Zeal sheet for actual UAV implementations on our in-house quad-copter codenamed T-Lion. In this section, more dimensions and different installation methods of Kyosho Zeal sheet were used and its effect on vibration reduction is studied.

### *5.1 Hardware Damper Design*

Flight tests are conducted with the different configurations in Table 1 aiming to verify the effects of each parameter

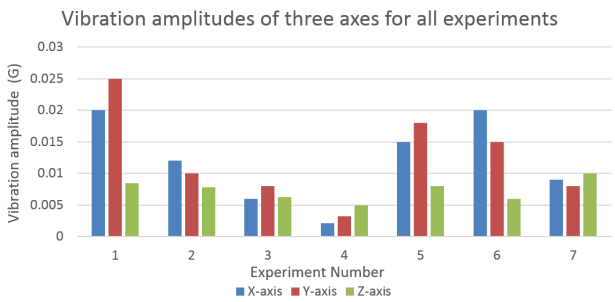


Figure 9: Kyosho Zeal sheet test results on three axes of UAV

| Experiment | Dimension (mm) | Installation | Contact |
|---|---|---|---|
| 1 | $12 \times 12 \times 5$ | Single | Less |
| 2 | $12 \times 12 \times 5$ | Single | More |
| 3 | $12 \times 12 \times 10$ | Single | More |
| 4 | $6 \times 6 \times 5$ | Single | More |
| 5 | $6 \times 6 \times 5$ | Clamped | More |
| 6 | $12 \times 12 \times 5$ | Clamped | More |
| 7 | $12 \times 12 \times 10$ | $45°$ | More |

Table 1: Kyosho Zeal sheet installation parameters

with regarding to Kyosho Zeal sheet performances.

Fig. 9 shows that the variations of vibration amplitudes of $x$-, $y$- and $z$-axis across different configurations of Kyosho Zeal sheets at 50 Hz. According to the results, experiment 4 has the best result in attenuating the vibration signals on T-lion UAV as the vibration amplitude is the lowest at 0.0021 G, 0.0032 G, and 0.005 G, comparing to vibration amplitude without any dampers at 0.08 G, 0.13 G and 0.17 G.

In general, the following guidelines for damper installation provide the best result for UAV vibration reduction:

1. More contact surface area of the damper is preferred;
2. Kyosho Zeal sheet should be installed vertically;
3. Even Length-Width-Height (LWH) ratio ($\approx 1:1:1$) gives the best results; and
4. Damper with smaller dimensions performs better for light mass damping.

### *5.2 Digital Low-Pass-Filter Design*

Actual flight experiment results show significant reductions in the vibration amplitudes (up to 97.1% reduction along the z-axis) with both damper and low-pass filter (cut-off frequency: 10 Hz) implemented. The illustration below (Fig. 10) shows that vibration signals could be amplified with damper alone, but the combined effect of both low-pass filter and damper will shift the system into isolation region, and this justifies the experiment results.

**IMAV2017-32**
https://www.imavs.org/pdf/imav.2017.32



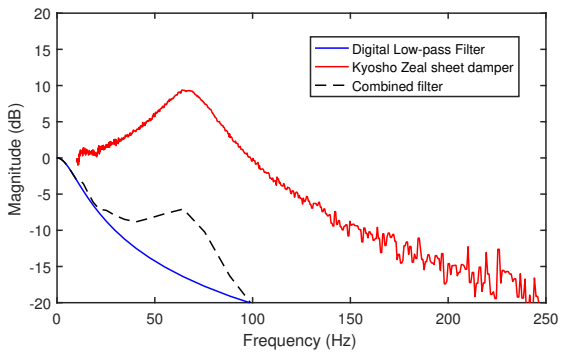


Figure 10: Combined frequency response of hardware damper and digital filter

Despite the high flexibility and softness of the chosen dampers, mechanical dampers show their limitations in damping light masses and at low frequency such as 50 Hz. On another hand, low-pass filter also has its limitation as its functional frequency range is much shorter than mechanical damper. Therefore, the use of low-pass filter is essential to lower amplified signal due to dampers while dampers are used to reject the high frequency vibrations due to the UAV structure.

## 6 Conclusion

This manuscript elaborates in detail the essential theoretical frameworks when considering anti-vibration measures on UAVs and how these can be used to improve on the current measures. Building on from this, criteria of damper selection for UAVs with light damping mass is established to act as guidelines for future practices.

With close examinations on vibration sources generated on T-lion UAV through both simulation and experimental results, it is shown that structural vibration contributes much higher vibration amplitude at higher frequencies comparing to motor vibration at lower frequency, addressing the importance of considering vibration attenuation for structural vibration when designing anti-vibration measures. Therefore, the relationships between different parameters of dampers and their damping effectiveness are closely evaluated through vibration tests, and the best performer, Kyosho Zeal sheet, further proves its effectiveness in minimizing structural vibrations at higher frequency, despite of creating slight signal amplification for motor vibration. This also indicates the limitation of mechanical damper in damping light mass at low disturbing frequency. Nonetheless, with both digital low-pass filter and Kyosho Zeal sheet, actual flight test shows up to 97.1% improvement on lowering the vibration amplitude. This addresses the significance of implementing both digital filter and mechanical damper for effective damping on UAVs.

Further studies can be done on vibration tests to investigate the pattern of how different parameters change with various masses and dimensions of the dampers in details, so that to predict its general performance and the optimal working range (in terms of damping mass and natural frequency) for each damper.

Lastly, this research work can be extended to other implications such as UAVs with different configurations and helicopter drones by making use of the frameworks and evaluation results provided in this paper.

## References

[1] K. Nonami, F. Kendoul, S. Suzuki, W. Wang, and D. Nakazawa. *Autonomous Flying Robots*. Springer, 2010.

[2] F. Wang, S. K. Phang, J. J. Ong, B. M. Chen, and T. H. Lee. Design and construction methodology of an indoor uav system with embedded vision. *Control and Intelligent Systems*, 40(1):22–32, 2012.

[3] S. K. Phang, F. Wang, K. Wang, S. Lai, and B. M. Chen. An effective method for autonomous localization and navigation in unknown indoor environment using mav. In *International Micro Air Vehicles Conference*, 2015.

[4] J. Langelaan and S. Rock. Navigation of small uavs operating in forests. In *AIAA Guidance, Navigation and Control Conference*, 2004.

[5] B. Sinopoli, M. Micheli, G. Donato, and J. T. Koo. Vision based navigation for an unmanned aerial vehicle. In *IEEE International Conference on Robotics and Automation*, 2001.

[6] T. H. Lee G. Cai, B. M. Chen. *Unmanned rotorcraft systems*. Springer, London/New York, 2011.

[7] V. Gavrilets, A. Shterenberg, M. A. Dahleh, and E. Feron. Avionics system for a small unmanned helicopter performing aggressive maneuvers. In *Digital Avionics Systems Conference*, 2000.

[8] A. Imam and R. Bicker. Design and construction of a small-scale rotorcraft uav system. *International Journal of Engineering Science and Innovative Technology*, 3(1):96–109, 2014.

[9] G. Cai, F. Lin, B. M. Chen, and T. H. Lee. Systematic design methodology and construction of uav helicopters. *Mechatronics*, 18(10):545–558, 2008.

[10] R. Simmons. Vibration isolation. *ASHRAE Journal*, pages 30–40, 2007.

[11] H. Fonseca. Displacement and force transmissibility in structures and multilayer supports with applications to vibration isolation. Master's thesis, Universidade Tecnica De Lisboa Instituto Superior Tecnico, Lisbon, Portugal, 2011.